Original

Evaluation of Homogeneity on Cone Beam Computed Tomography Imaging with Flat Panel Detector

Noriyuki Sugino

Department of Oral and Maxillofacial Radiology, Matsumoto Dental University School of Dentistry, Shiojiri, 399-0781 Japan
(Accepted for publication, July 30, 2009)

Abstract: Cone beam computed tomography (CBCT) with a flat panel detector can provide more precise and fine images compared to that with an image intensifier which have been used previously. Measurement of the length clearly varies among different measurement regions on the images of CBCT with an image intensifier. However, little is known whether measurement of the length on the images of CBCT with a flat panel detector varies as well or uniform. The objective of this study was, therefore, to analyze the homogeneity of the measurement of the length on the images of the CBCT with a flat panel detector.

The results demonstrated that both short- and long-term reproducibility of measurement of the length on the CBCT images of the x-ray mesh gauge was less than 1.5%. The non-uniformity of measurement of the length on the CBCT images was less than 2% between any of two regions. The non-uniformity of measurement of the length on the CBCT images with ϕ60mm×h60mm exposed area was almost constant at any regions independent of the tube current. That on the CBCT images with ϕ40mm×h40mm exposed area varied randomly.

The non-uniformity of measurement of the length varied randomly on the CBCT images with small exposed area; however, this was considerably small and negligible. The results suggest that measurement of the length on the images of CBCT with a flat panel detector may be substantially uniform at any regions in comparison with that on the images of CBCT with an image intensifier.

Key words: Computed tomography, Cone beam, Flat panel detector, Homogeneity

Introduction

It is very important for the dentists to evaluate the quantity and quality of alveolar bone on dental implant placement, the relation of impacted tooth with surrounding tissues such as mandibular canal and sinus floor on tooth extraction, root canal shape on endodontics treatments and so on. Generally, intraoral and panoramic radiographs are widely used for these dental treatments in general dental practise. However, it is reasonable that relatively insufficient information may be obtained by these radiographs because it can present only two-dimensional information of maxillofacial regions. Therefore, the conventional x-ray computed tomography (CT) that was widely used in medical field and can provide three-dimensional information have been applied in dental field since late 1980s, especially for planning the dental implant placements[1].

Recently, multi-slice CT (MSCT) or multi-detector CT (MDCT) with a high radiation exposure had been introduced in dental field instead of single-slice conventional CT. This may contribute to the increase of radiation-induced cancer incidence,

especially in Japan[2]. Radiation exposure accompanied by MSCT should be reduced as possible in children as well as women over the world[3]. The new recommendation of the International Commission on Radiological Protection (ICRP) in 2007 added tissue-weighting factor for salivary gland and brain that are related to the incidence of stochastic effect due to radiation exposure in dental field. At the viewpoint of the reduction of radiation exposure, cone beam CT (CBCT) was newly developed for dental clinical applications at the late of 2000s[4,5].

CBCT possesses some advantages such as having higher detection of subtle hard tissue like bone and tooth and spatial resolution as well as assuring the decrease of radiation exposure compared to medical MDCT[6,7]. CBCT uses a conical type of x-ray beam and curved or flat two-dimensional x-ray detector. In the early type of CBCT, an image intensifier (I.I.), which sometimes used for a C-arm or fluoroscope in medical field, was used as the detector of x-ray[8]. I.I. has a high sensitive semiconductor that converts the last electrical signal[9]. However, an unstable signal due to curved shaped I.I. detector produced the non-uniformity of measurement of the distance on the images of CBCT. Ohtsuka has developed an original software to correct the non-uniformity of measurement of the distance on the image of cineradiography with the I.I., resulting in the reduction of the non-

Correspondence to: Dr. Noriyuki Sugino, Department of Oral and Maxillofacial Radiology, Matsumoto Dental University School of Dentistry, Shiojiri, 399-0781 Japan. E-mail: b0211nsugi@po.mdu.ac.jp, Tel & Fax: +81-263-51-2096

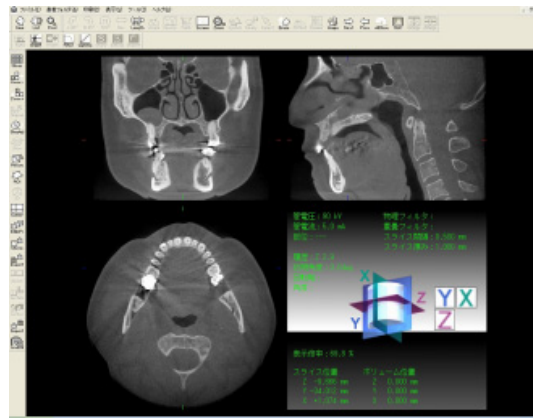Figure 1.Cone beam computed tomography (CBCT).

Figure 2. Coronal image (upper left), sagittal image (upper right) and axial image (lower left) of CBCT.

Figure 3. The phantom consisted of four pieces of water equivalent material.
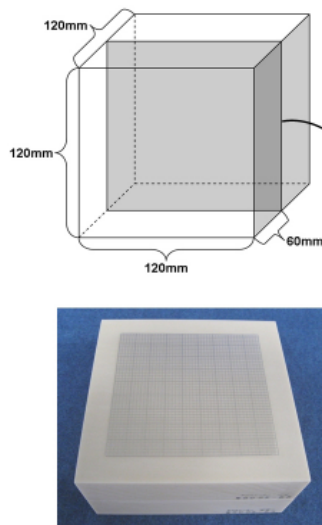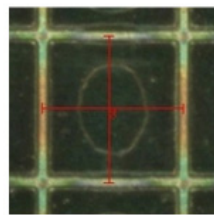

Figure 4. The stainless steel x-ray mesh gauge embedded in the phantom.

Figure 5. The x-ray mesh gauge (A) and it's microscope image (B).

Figure 6. The phantom and a level.

uniformity[9]. On CBCT as well, it is very important to sustain the homogeneity of measurement of the distance at any regions on CBCT image in clinical applications[10].

Recently, flat panel detector (FPD) with both fluorescent screen and semiconductor had been integrated in CBCT. FPD has succeeded in holding down the fluctuation that occurs with I.I. On FPD, the x-ray signal is easily converted into digital signal with lesser fluctuation. Therefore, high spatial resolution is obtained on FPD without deterioration of the image due to fluctuation. FPD has also higher image contrast. The contrast resolution of I.I. is 8 bit with 256 gradations. On FPD, this is expanded to 12 bit with 4096 gradations, contributing to high sensitivity for the detection of a few contrasts on the image.

To date, many researchers have been investigating the precision of the measurement of the distance on the images on CBCT alone or comparing that on both CBCT and MDCT. They finally conclude that CBCT has better precision for the measurement than MDCT[11-16]. However, little is known whether measurement values of the distance between two sites are homogeneous at any region of the CBCT image. The objective of this study was to analyze the homogeneity of measurement of the distance on CBCT image with FPD.

Materials and Methods

CBCT equipment

I used in this study the recently-developed CBCT (Morita Co., Kyoto) with FPD, the designated 3D Accuitomo type F17. This consists of a chair for the subjects and two rotated arms with gate-shaped. One arm is equipped with the x-ray tube and the other arm the FPD (Fig. 1). Tomography shape obtained by CBCT is cylindrical. The 5 size of the cylinder can be selected in this CBCT: $\phi40\,mm\times h40\,mm$, $\phi60\,m\times h60\,m$, $\phi80\,mm\times h80\,mm$, $\phi100mm\times h100mm$, and $\phi170mm\times h120mm$. Prior to taking the CBCT images, the lateral and frontal images of the subjects are obtained to determine the precise position of the imaging area. Thereafter, the cursor is adjusted to the centre of the imaging area,
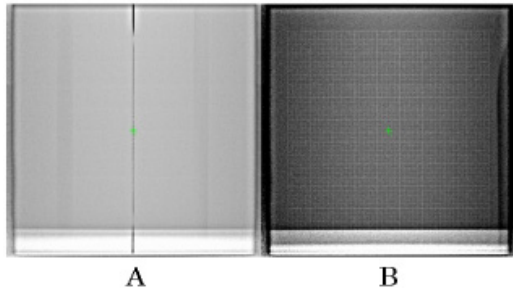
Figure 7. Lateral (A) and frontal (B) x-ray images of the x-ray mesh gauge embedded in the phantom.
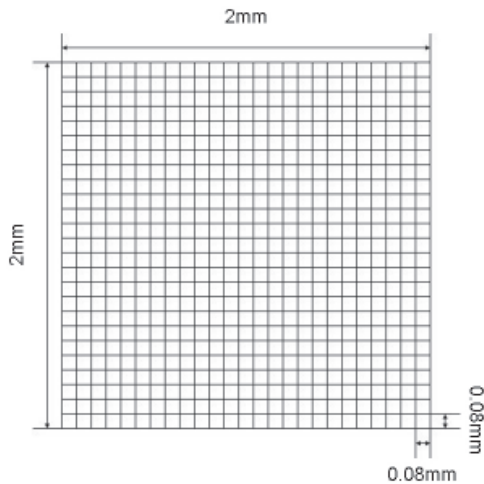

Figure 9. Ideal pixel pattern of the x-ray mesh gauge in the area of CBCT; the size of the measurement is 40×40.
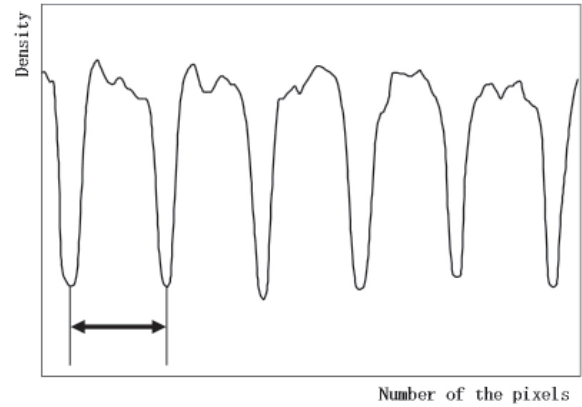

Figure 8. Number of pixels between the neighboring two peaks (black arrow) of the density profile of the x-ray mesh gauge was considered as the distance.
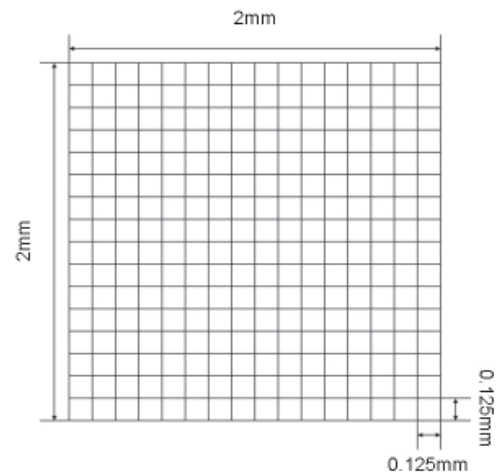

Figure 10. Ideal pixel pattern of the x-ray mesh gauge in the area of CBCT; the size of the measurement is 60×60.

where the dentists want to take, on these lateral and frontal images. After the determination of the precise position, the arms rotate around the subject and 590 x-ray tomography images are automatically obtained with the time of 17.5 seconds.

The i-VIEW software (Morita Co., Kyoto) was used to obtain and analyze three-dimensional reconstruction tomography images (horizontal, sagittal and frontal images) of CBCT (Fig. 2). Sizes of the voxel were between 0.080mm and 0.250mm according to the size of the cylindrical tomography shape obtained by CBCT.

Experimental phantom

The cube shape phantom with a size of 120mm×120mm× 120mm was constructed as the phantom for the study using plane board tough water phantom WE type (Kyoto Kagaku Co., Kyoto). The density of this phantom (1.017g/cm^3) was almost equal to that of the water (Fig. 3). In addition, I used stainless steel x-ray mesh gauge with a size of 90mm×90mm× 0.1mm (DENTECH, Tokyo) and with a grid of 2mm interval. This was placed in the centre of the cube shape experimental phantom (Fig. 4). The interval of the grid on x-ray mesh gauge was confirmed using a microscope before the study (Fig. 5).

Parameters of the CBCT imaging

The tube voltage and total filtration were 90kV and 3.1mmAl, respectively. In addition, four typical parameters of the tube current and the tomography imaging volume were used in this study: 5mA and φ40mm×h40mm, 7mA and φ40mm×h40mm, 5mA and φ60mm×h60mm, and 7mA and φ60mm×h60mm. Prior to taking CBCT of the phantom, a levelling instrument was used to confirm whether top of the phantom is almost parallel to the floor (Fig. 6). The x-ray mesh gauge was placed parallel or perpendicular to the FPD before the CBCT exposure (Fig. 7).

The X (frontal) and Y (lateral) plane images of the x-ray mesh gauge were obtained for parameters (4 current tube and imaging volumes) on CBCT. The images were taken 3 times within a day with an interval of 4 hours. Additionally, the images were taken 3 times with an interval of 1 week.

Calculation of the profile

In the imaging area of φ40mm×h40mm, the slice thickness and interval were 0.080mm and 0.080mm, respectively. In the imaging

Figure 11. Five ROIs in measuring the distance; upper left (UL), upper right (UR), lower left (LL), lower right (LR), and the center (CC) on the size of the measurement at 40×40.
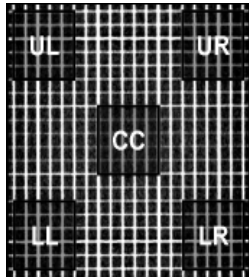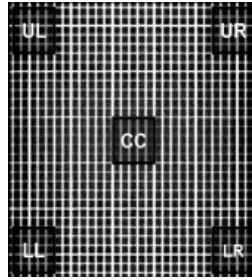

Figure 12. Five ROIs in measuring the distance; upper left (UL), upper right (UR), lower left (LL), lower right (LR), and the center (CC) on the size of the measurement at 60×60.
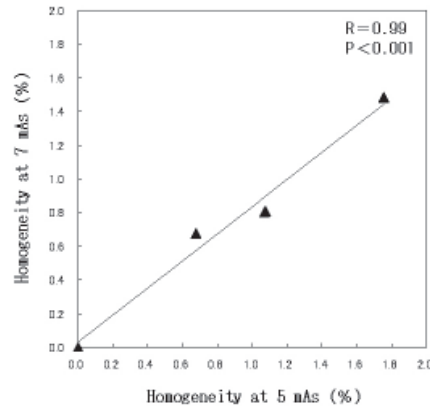

Figure 13. The relationship between the heterogeneity of measuring the distance when exposed at 5mAs and 7mAs in horizontal direction on X plane at 60×60.
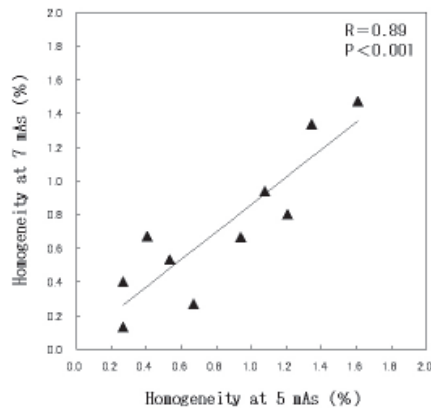

Figure 14. The relationship between the heterogeneity of measuring the distance when exposed at 5mAs and 7mAs in vertical direction on X plane at 60×60.

Figure 15. The relationship between the heterogeneity of measuring the distance when exposed at 5mAs and 7mAs in horizontal direction on Y plane at 60×60.

area of ϕ60mm×h60mm, the slice thickness and interval were 0.125mm and 0.125mm, respectively Therefore, the voxel size in the imaging area of ϕ40mm×h40mm and ϕ60mm×h60mm, respectively, were 0.080mm and 0.125mm in each side. Data was stored with bitmap and incorporated into the software for image analysis (Scion Image Beta 4.02, Scion Corporation, USA).

Measurement of the distance on the CBCT image and measurement region

Number of pixels between peak values representing 1 grid interval of the x-ray mesh gauge on density profile of the CBCT image was considered as the distance between the grids (Fig. 8). If there was no noise including x-ray quantum noise, the distance between the grids is 25 pixels in the area of ϕ40mm×h40mm (Fig. 9) and 16 pixels in the area of ϕ60mm×h60mm (Fig. 10).

Measurements of the mean distance were performed horizontally and vertically in 5 different regions: central (CC), upper left (UL), upper right (UR), lower left (LL), and lower right (LR) (Figs. 11 and 12). These measurements were performed on

X and Y plane images as well.

Data analysis

The coefficient of variation of 3 data obtained within a day was defined as a short-term reproducibility of the measurement of the distance. The coefficient of variation of 3 data obtained with an interval of 1 week was defined as a long-term reproducibility of measurement of the distance.

One-way analysis of covariance was performed to evaluate the homogeneity in measurement of the distance among 5 regions on CBCT images. Homoscedasticity was analyzed by Levene statistic. Bonferroni correction for multiple test was done when homoscedastic was verified, and Tamhane's test was applied when homoscedastic were not verified. Data analyses were performed using the Statistical Package for the Social Sciences (SPSS; version 8.0; SPSS Inc., Chicago, IL). P-values < 0.05 were considered statistically significant.

Absolute difference values of the measured distances between two different areas (CC-UL, CC-UR, CC-LL, CC-LR, UL-UR,

Figure 16. The relationship between the heterogeneity of measuring the distance when exposed at 5mAs and 7mAs in vertical direction on Y plane at 60×60.
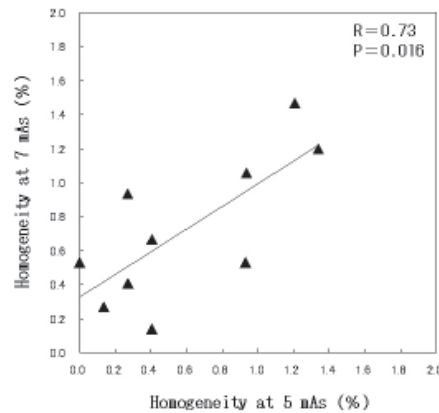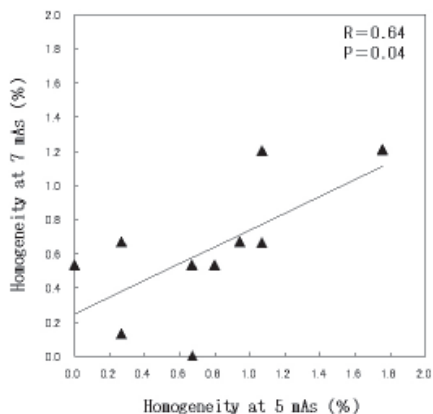

Figure 17. The relationship between the heterogeneity of measuring the distance when exposed at 5mAs and 7mAs in horizontal direction on X plane at 40×40.

Figure 18. The relationship between the heterogeneity of measuring the distance when exposed at 5mAs and 7mAs in vertical direction on X plane at 40×40.
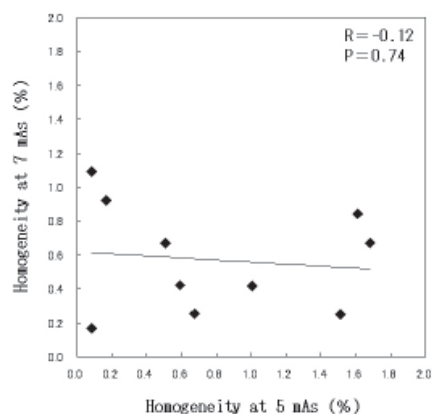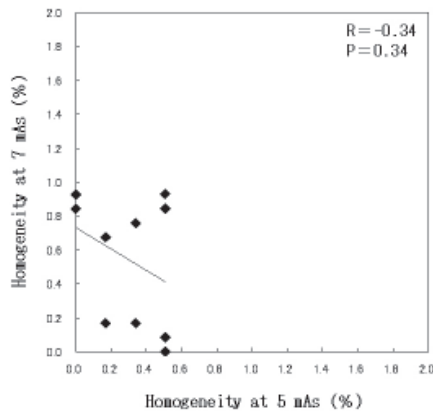

Figure 19. The relationship between the heterogeneity of measuring the distance when exposed at 5mAs and 7mAs in horizontal direction on Y plane at 40×40.
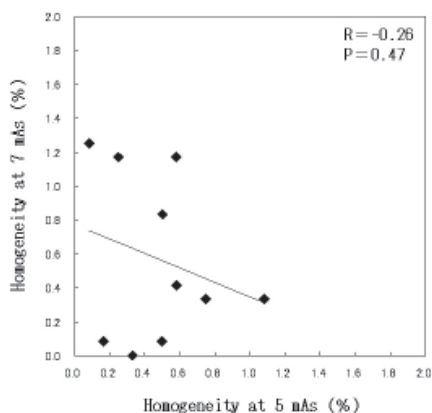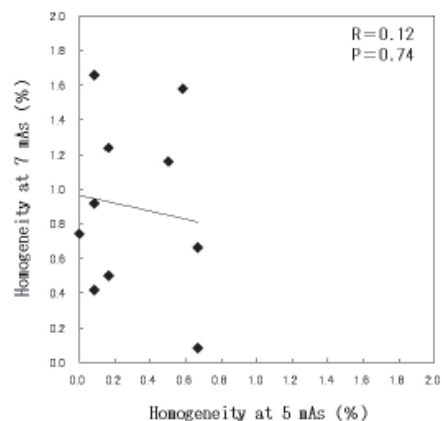

Figure 20. The relationship between the heterogeneity of measuringthe distance when exposed at 5mAs and 7mAs in vertical direction on Y plane at 40×40

UL-LL, UL-LR, UR-LL, UR-LR, LL-LR) were considered as an index representing non-uniformity of the distance on CBCT images.

Non-uniformity of the distance on CBCT images with a tube current of 5mA was compared with a tube current of 7mA in order to investigate the effect of tube current on non-uniformity of the distance.

Results

In the imaging area of ϕ40mm×h40mm, short-term reproducibility was less than 1.24% for horizontal direction on X plane with a tube current of 5mA (Table 1) and less than 1.09% for vertical direction on X plane with a tube current of 7mA (Table 2).

In the imaging area of ϕ60mm×h60mm, short-term reproducibility was less than 0.66% for vertical direction on X plane with a tube current of 5mA (Table 3) and less than 1.18% for horizontal direction on X plane with a tube current of 7mA (Table 4).

In the imaging area of ϕ40mm×h40mm, long-term reproducibility was less than 0.58% for horizontal direction on X plane with a tube current of 5mA (Table 5) and less than 0.58% for vertical direction on Y plane with a tube current of 7mA (Table 6).

Table 1. short-term reproducibility (within a day) of measuring the distance between two regions of interest (ROIs) in the area of cone beam computed tomography (CBCT) at 5 mA; the size of the measurement is 40x40.

Region of the measurement	X plane horizontal	X plane vertical	Y plane horizontal	Y plane vertical
UR	0.15	0.37	0.21	1.02
UR	0.30	0.88	0.25	0.65
CC	0.15	0.25	0.05	0.55
LL	0.13	0.38	0.14	0.78
LR	1.24	1.05	0.32	0.92
				%

Table 2. short-term reproducibility (within a day) of measuring the distance between two regions of interest(ROIs) in the area of cone beam computed tomography (CBCT) at 7mA; the size of the measurement is 40x40.

Region of the measurement	X plane horizontal	X plane vertical	Y plane horizontal	Y plane vertical
UL	0.68	0.63	0.08	0.13
UR	0.75	0.58	0.00	0.17
CC	0.72	1.09	0.13	0.29
LL	0.80	0.60	0.13	0.34
LR	0.05	0.22	0.08	0.30
				%

Table 3. short-term reproducibility (within a day) of measuring the distance between two regions of interest(ROIs) in the area of cone beam computed tomography (CBCT) at 7mA; the size of the measurement is 60x60.

Region of the measurement	X plane horizontal	X plane vertical	Y plane horizontal	Y plane vertical
UL	0.54	0.40	0.35	0.14
UR	0.00	0.14	0.55	0.13
CC	0.00	0.20	0.21	0.66
LL	0.08	0.15	0.58	0.08
LR	0.00	0.16	0.40	0.23
				%

Table 4. short-term reproducibility (within a day) of measuring the distance between two regions of interest(ROIs) in the area of cone beam computed tomography (CBCT) at 7mA; the size of the measurement is 60x60.

Region of the measurement	X plane horizontal	X plane vertical	Y plane horizontal	Y plane vertical
UL	0.43	0.82	0.68	0.28
UR	0.00	0.82	0.40	0.66
CC	0.00	0.13	0.40	0.27
LL	0.08	0.85	0.60	0.68
LR	0.00	0.34	1.18	0.51
				%

Table 5. Long-term reproducibility (day a day) of measuring the distance between two ROIs in the area of CBCT at 5mA; the size of the measurement is 40 x40.

Region of the measurement	X plane horizontal	X plane vertical	Y plane horizontal	Y plane vertical
UL	0.11	0.36	0.15	0.04
UR	0.42	0.23	0.14	0.08
CC	0.02	0.35	0.02	0.03
LL	0.06	0.58	0.18	0.07
LR	0.17	0.42	0.15	0.09
				%

Table 6. Long-term reproducibility (day a day) of measuring the distance between two ROIs in the area of CBCT at 7 mA; the size of the measurement is 40 x40.

Region of the measurement	X plane horizontal	X plane vertical	Y plane horizontal	Y plane vertical
UL	0.35	0.34	0.55	0.36
UR	0.11	0.27	0.50	0.58
CC	0.06	0.04	0.14	0.04
LL	0.35	0.34	0.53	0.50
LR	0.28	0.14	0.52	0.51
				%

In the imaging area of ϕ60mm×h60mm, long-term reproducibility was less than 0.87% for horizontal direction on Y plane with a tube current of 5mA (Table 7) and less than 1.05% for horizontal direction on Y plane with a tube current of 7mA (Table 8).

There was significant difference in the measured distance in the imaging area of ϕ40mm×h40mm for vertical direction on Y plane (P=0.02) (Table 9). However, multiple comparisons revealed significant difference between only UL and LL regions (P=0.04).

In the imaging area of ϕ40mm×h40mm, absolute difference values was less than 1.68% for horizontal direction on X plane with a tube current of 5mA (Table 10) and less than 1.66% for vertical direction on Y plane with a tube current of 7mA (Table 11).

In the imaging area of ϕ60mm×h60mm, absolute difference values was less than 1.75% for vertical direction on Y plane with a tube current of 5mA (Table 12) and less than 1.49% for horizontal direction on X plane with a tube current of 7mA (Table 13).

In the imaging area of ϕ60mm×h60mm, non-uniformities on CBCT images with a tube current of 5mA tended to be somewhat correlated with that on CBCT images with a tube current of 7mA

Table 7. Long-term reproducibility (day a day) of measuring the distance between two ROIs in the area of CBCT at 5 mA; the size of the measurement is 60 x60.

Region of the measurement	X plane horizontal	X plane vertical	Y plane horizontal	Y plane vertical
UL	0.22	0.75	0.62	0.65
UR	0.34	0.75	0.44	0.58
CC	0.38	0.27	0.45	0.25
LL	0.32	0.67	0.87	0.81
LR	0.44	0.60	0.44	0.72
				%

Table 8. Long-term reproducibility (day a day) of measuring the distance between two ROIs in the area of CBCT at 7 mA; the size of the measurement is 60 x60.

Region of the measurement	X plane horizontal	X plane vertical	Y plane horizontal	Y plane vertical
UL	0.27	0.45	0.72	0.66
UR	0.39	0.27	0.33	0.50
CC	0.38	0.21	0.41	0.34
LL	0.05	0.31	1.05	0.57
LR	0.29	0.58	0.74	0.69
				%

Table 9. Evaluetion of the homogeneity of measuring the distance.

conditions	X plane horizontal	X plane vertical	Y plane horizontal	Y plane vertical
5ml φ40mm×H40mm	0.07	0.75	0.93	0.93
7ml φ40mm×H40mm	0.22	0.46	0.34	0.02
5ml φ60mm×H60mm	0.12	0.30	0.51	0.55
7ml φ60mm×H60mm	0.23	0.24	0.33	0.61
				p-Value

Table 10. Non-uniformity of measuring the distance been two ROIs in the area of CBCT at 5mAs; the size of the measurement is 40x40.

Two ROIs	X plane horizontal	X plane vertical	Y plane horizontal	Y plane vertical
CC-UL	0.08	1.08	0.51	0.08
CC-UR	0.68	0.50	0.34	0.58
CC-LL	0.17	0.33	0.51	0.08
CC-LR	1.68	0.58	0.00	0.08
UL-UR	0.59	0.58	0.17	0.67
UL-LL	0.08	0.75	0.00	0.17
UL-LR	1.61	0.50	0.51	0.00
UR-LL	0.51	0.17	0.17	0.50
UR-LR	1.01	0.08	0.34	0.67
LL-LR	1.51	0.25	0.51	0.17
				%

Table 11. Non-uniformity of measuring the distance been two ROIs in the area of CBCT at 7mAs; the size of the measurement is 40x40.

Two ROIs	X plane horizontal	X plane vertical	Y plane horizontal	Y plane vertical
CC-UL	0.17	0.33	0.00	1.66
CC-UR	0.25	0.08	0.17	1.58
CC-LL	0.92	0.00	0.84	0.42
CC-LR	0.67	1.17	0.93	0.92
UL-UR	0.42	0.42	0.17	0.08
UL-LL	1.09	0.34	0.84	1.24
UL-LR	0.84	0.83	0.93	0.74
UR-LL	0.67	0.08	0.67	1.16
UR-LR	0.42	1.25	0.76	0.66
LL-LR	0.25	1.17	0.08	0.50
				%

Table 12. Non-uniformity of measuring the distance been two ROIs in the area of CBCT at 7mAs; the size of the measurement is 60x60.

Two ROIs	X plane horizontal	X plane vertical	Y plane horizontal	Y plane vertical
CC-UL	1.75	0.53	1.34	0.67
CC-UR	0.68	1.61	0.13	0.27
CC-LL	0.68	0.27	0.40	0.00
CC-LR	0.68	1.20	0.40	1.07
UL-UR	1.08	1.08	1.20	0.94
UL-LL	1.08	0.27	0.94	0.67
UL-LR	1.07	0.67	0.93	1.75
UR-LL	0.00	1.34	0.27	0.27
UR-LR	0.00	0.40	0.27	0.80
LL-LR	0.00	0.94	0.00	1.07
				%

independent of the differences in the plane (X or Y) and direction (vertical or horizontal) (Figs. 13-16). On the other hand, in the imaging area of φ40mm×h40mm, the non-uniformity of measurement of the distance varied randomly. There was no association in non-uniformities on CBCT images between using 5mA and 7mA (Fig. 17-20).

Discussion

In this study, short- and long-term reproducibility of measurement of the distance on CBCT images was less than 1.5%, indicating sufficient reproducibility. Basically, if the reproducibility is poor, the evaluation of the homogeneity of measurement of the distance on the CBCT images is not meaningful. That is why we first confirmed the short- and long-term reproducibility in this

Table 13. Non-uniformity of measuring the distance been two ROIs in the area of CBCT at 7mAs; the size of the measurement is 60x 60.

Two ROIs	X plane horizontal	X plane vertical	Y plane horizontal	Y plane vertical
CC-UL	1.49	0.53	1.20	0.00
CC-UR	0.68	1.47	0.27	0.67
CC-LL	0.68	0.13	0.14	0.54
CC-LR	0.68	0.80	0.67	1.20
UL-UR	0.81	0.94	1.47	0.67
UL-LL	0.81	0.40	1.06	0.54
UL-LR	0.80	0.27	0.53	1.21
UR-LL	0.00	1.34	0.41	0.13
UR-LR	0.00	0.67	0.94	0.53
LL-LR	0.00	0.67	0.53	0.67

%

study. Hildebolt et al. evaluated the alveolar bone loss on intra-oral radiographs with a coefficient of variance of 2.3% using a computer-intensive method[17]. It may be difficult to compare the results with other data regarding reproducibility in clinical studies; however, the results suggest that measurement of the distance on CBCT image may be relatively reproducible in clinical practice. The alveolar bone measurement[14], pre-surgical assessment of implant site[18] temporomandibular joint[19] have recently investigated by CBCT. Although the data were obtained by phantom, the results also suggest that change of measurement of the distance on CBCT might be ideally detected up to 4.1% $(1.5 \times 1.96 \times \sqrt{2}$ between the exemainations.

After the early 1990s, whole body CT used in the medical field have been applied in general dental practice, especially for pre-surgical assessment of implant placement. CT value (HU) obtained by medical CT is considered an useful indicator in assessing bone quantity and quality, although CT value easily change due to some factors like quantum noise[20]. However, since medical CT including MDCT provides high radiation dose to the patients, resulting in the increase of radiation-induced cancer incidence, CBCT that provides relative low radiation dose have been developed and rapidly spread in clinical dental practice over the world. However, in CBCT with I.I. homogeneity of measurement of the distance could not be maintained[10] because of complex structure contributing to fluctuation effect. To improve this problem, CBCT with FPD that has simple structure to convert x-ray signal into digital signal have been developed. However, since little is known whether homogeneity of measurement of the distance on CBCT image is improved compared with CBCT with I.I., I investigated the homogeneity of measurement of the distance on CBCT image with FPD.

The current study found a significant difference only between vertical directions of UL and LL in imaging area of φ40mm×h40mm on Y-plane; however, it is likely that this may be caused by chance finding because no significant differences were found in other situations. Therefore, I can indicate good homogeneity of measurement of the distance on CBCT image with FPD. Absolute difference values among the 5 areas on CBCT image was less than 2% so that this also indicate good homogeneity of measurement of the distance on CBCT image with FPD. If the distance from the alveolar crest to the mandibular canal was 10mm, the results indicate that distance measured on CBCT image was between 9.8mm and 10.2mm at any regions. This does not seem to be a clinical problem.

In the imaging area of φ60mm×h60mm, non-uniformities on CBCT images with a tube current of 5mA were correlated with that on CBCT images with a tube current of 7mA independent of other parameters. On the other hand, in the imaging area of φ40mm×h40mm, the non-uniformity of measurement of the distance varied randomly. The main cause of the noise is the x-ray quantum mottle and system noise. It is likely that these may influence on the phenomena in the imaging area of φ40mm×h40mm. However, since the non-uniformity of measurement of the distance in the imaging area of φ40mm×h40mm is considerably small, these phenomena do not influence on the results in clinical use.

CBCT with FDP will rapidly spread in the near future in dental field as well as medical field. Evaluation of both reproducibility and precision are very important when investigators or clinicians want to apply CBCT[21]. Caution should be noted when interpreting the results if this information is not obtained. The results indicated the high reproducibility and good homogeneity for measurement of the distance on CBCT images; however, further investigation would be necessary to clarify the usefulness of CBCT with FPD in clinical dental practice. in conclusions, the reproducibility of measurement of the distance on CBCT images with FPD was less than 1.5%. Homogeneity of measurement of the distance among 5 areas (center, upper right, lower right, upper left and lower left) on CBCT images was good. Absolute difference values of the measured distance between any two regions on CBCT images were less than 2%. When the imaging area is small, non-uniformity of measurement of the distance on CBCT images varied randomly. However, this variation was considerably small. I conclude that it can be measured the distance with good reproducibility and sufficient homogeneity at any regions on CBCT with FDP.

References

1. Almog DM, Benson BW, Wolfgang L, Frederiksen NL and Brooks SL. Computerized tomography-based imaging and surgical guidance in oral implantology. J Oral Implantol 32: 14-8, 2006

2. Berrington de González A and Darby S. Risk of cancer from diagnostic X-rays: estimates for the UK and 14 other countries. Lancet 363: 345-51, 2004

3. Brenner DJ and Hall EJ. Computed tomography—an increasing source of radiation exposure. New Eng J Med 357: 2277-84, 2007

4. Arai Y, Tammisalo E, Iwai K, Hashimoto K and Shinoda K. Development of a compact computed tomographic apparatus for dental use. Dentomaxillofac Radiol 28: 245-8, 1999

5. Terakado M, Hashimoto K, Arai Y, Honda M, Sekiwa T and Sato H. Diagnostic imaging with newly developed ortho cubic super-high resolution computed tomography (Ortho-CT). Oral Surg Oral Med Oral Pathol Oral Radiol Endod 89: 509-18, 2000

6. Kim S, Yoshizumi TT, Toncheva G, Yoo S and Yin FF. Comparison of radiation doses between cone beam CT and multi detector CT: TLD measurements. Radiat Prot Dosimetry 132: 339-345, 2008

7. Yoshida Y, Honda E, Tomotake Y, Nagao D and Ichikawa T. Evaluation of patient dose in imaging using a cone-beam CT for dental use. J Soc Oral Implantol 20: 280-6, 2007

8. Arai Y, Hashimoto K, Iwai K and Shinoda K. Fundamental efficiency of limited cone-beam x-ray CT (3DX multi image micro CT) for practical use. Dent Radiol 40: 145-54, 2000

9. Ohtsuka M. Reduction of patient dose and improvement of measurement accuracy in radiographic swallowing studies. Dent Radiol 44: 1-15, 2004

10. Sugino N, Uchida K, Shiojima M. Fundamental evaluation of standard on cone beam computed tomography (3DX). Dent Radiol 47: 116, 2007

11. Ludlow JB, Laster WS, See M, Bailey LJ and Hershey HG. Accuracy of measurements of mandibular anatomy in cone beam computed tomography images. Oral Surg Oral Med Oral Pathol Oral Radiol Endod 103: 534-42, 2007

12. Mischkowski RA, Pulsfort R, Ritter L, Neugebauer J, Brochhagen HG, Keeve E and Zöller JE. Geometric accuracy of a newly developed cone-beam device for maxillofacial imaging. Oral Surg Oral Med Oral Pathol Oral Radiol Endod 104: 551-9, 2007

13. Suomalainen A, Vehmas T, Kortesniemi M, Robinson S and Peltola J. Accuracy of linear measurements using dental cone beam and conventional multislice computed tomography. Dentomaxillofac Radiol 37: 10-7, 2008

14. Loubele M, Van Assche N, Carpentier K, Maes F, Jacobs R, van Steenberghe D and Suetens P. Comparative localized linear accuracy of small-field cone-beam CT and multislice CT for alveolar bone measurements. Oral Surg Oral Med Oral Pathol Oral Radiol Endod 105: 512-8, 2008

15. Veyre-Goulet S, Fortin T and Thierry A. Accuracy of linear measurement provided by cone beam computed tomography to assess bone quantity in the posterior maxilla: a human cadaver study. Clin Implant Dent Relat Res 10: 226-30, 2008

16. Stratemann SA, Huang JC, Maki K, Miller AJ and Hatcher DC. Comparison of cone beam computed tomography imaging with physical measures. Dentomaxillofac Radiol 37: 80-93, 2008

17. Hildebolt CF, Brunsden B, Yokoyama-Crothers N, Pilgram TK, Townsend KE, Vannier MW and Shrout MK. Comparison of reliability of manual and computer-intensive methods for radiodensity measures of alveolar bone loss. Dentomaxillofac Radiol 27: 245-50, 1998

18. Hatcher DC, Dial C and Mayorga C. Cone beam CT for pre-surgical assessment of implant sites. J Calif Dent Assoc 31: 825-33, 2003

19. Honey OB, Scarfe WC, Hilgers MJ, Klueber K, Silveira AM, Haskell BS and Farman AG. Accuracy of cone-beam computed tomography imaging of the temporomandibular joint: comparisons with panoramic radiology and linear tomography. Am J Orthod Dentofacial Orthop 132: 429-38, 2007

20. Taguchi A, Tanimoto K, Ogawa M, Sunayashiki T and Wada T. Effect of size of region of interest on precision of bone mineral measurements of the mandible by quantitative computed tomography. Dentomaxillofac Radiol 20: 25-9, 1991

21. Mol A and Balasundaram A. In vitro cone beam computed tomography imaging of periodontal bone. Dentomaxillofac Radiol 37: 319-24, 2008